Plasticization of poly(methyl methacrylate) (PMMA) networks by supercritical carbon dioxide

S. K. Goel and E. J. Beckman*

Chemical Engineering Department, University of Pittsburgh, Pittsburgh, PA 15260, USA

(Received 20 December 1991; revised 27 April 1992)

It has been shown by a number of authors that supercritical carbon dioxide is an extremely efficient plasticizer for amorphous, carbonyl-containing polymers. In this paper, we have examined the plasticization of poly(methyl methacrylate) (PMMA) networks by CO_2 as a function of pressure using dielectric measurements. Results show that the degree of plasticization increases rapidly at pressures up to approximately 1200 psig (8.274 MPa), levelling off (and possibly decreasing) at higher pressures. This phenomenon is possibly due to the counteracting effects of pressure on free volume and CO_2 sorption. The experimental trends are consistent with predictions of free volume in CO_2/PMMA mixtures derived from a modified lattice model.

(Keywords: plasticization; poly(methyl methacrylate); networks)

INTRODUCTION

Supercritical fluids (SCF), materials at temperatures and pressures above their critical values, are of great technological interest because they exhibit properties which lie between those of conventional liquids and gases[1]. Further, the physical properties of materials (density, solubility parameter, viscosity, dielectric constant) at temperatures close to the critical point can be varied over a wide range through adjustments to the pressure. This allows the solvating power of a supercritical solvent to be effectively tuned using pressure, a characteristic which has led to the development of supercritical fluid processes where a single component is cleanly extracted from a complex matrix, or where a mixture is fractionated via pressure-programming.

It has been shown previously that supercritical carbon dioxide ($T_c = 31°C$, $P_c = 72.8$ atm (7.38 MPa)) is an extremely efficient plasticizer for polymers[2-11], owing to its liquid-like density, high diffusivity and low molecular weight. For example, Wang *et al.*[5] calculated the glass transition of polystyrene swollen by supercritical CO_2 using the Williams–Landel–Ferry (WLF) equation and creep compliance measurements (from which a shift factor was derived); the results showed that CO_2 reduces the T_g from 100°C to as low as 35°C at 200 atm (20.26 MPa). Interestingly, Wang's results suggested that the glass transition exhibits a minimum as pressure increases, owing to the counteracting effects of pressure on free volume and on CO_2 sorption. More recent work by Wissinger and Paulaitis[6], also using creep compliance measurements, shows a monotonic decrease in T_g of polystyrene as CO_2 pressure increases from 1 to 60 atm (0.1 to 6.08 MPa). Differential scanning calorimetry (d.s.c.) measurements by Chiou *et al.*[8] at pressures up to 20 atm (2.03 MPa) are conistent with these results.

Whereas CO_2 is a relatively poor solvent for polystyrene, this gas shows a strong affinity for acrylate and methacrylate polymers[12]. Chiou *et al.* measured the sorption of CO_2 by poly(methyl methacrylate) (PMMA) and also the resulting T_g depression using d.s.c.[8]. At pressures up to approximately 40 atm (4.06 MPa), T_g was observed to decrease monotonically with pressure. Experiments at higher pressures by Wissinger and Paulaitis[6], using the previously mentioned creep compliance method, reveal rather different trends. Whereas T_g drops monotonically with increasing absorbed CO_2 weight fraction, if T_g is plotted against CO_2 pressure then there appears to exist a pressure (approximately 40 atm (4.06 MPa)) above which the polymer adopts a liquid state at all temperatures above room temperature (and possibly considerably below room temperature also). This somewhat surprising phenomenon can be explained by the use of *Figure 1*.

If a situation is assumed where a mass of amorphous

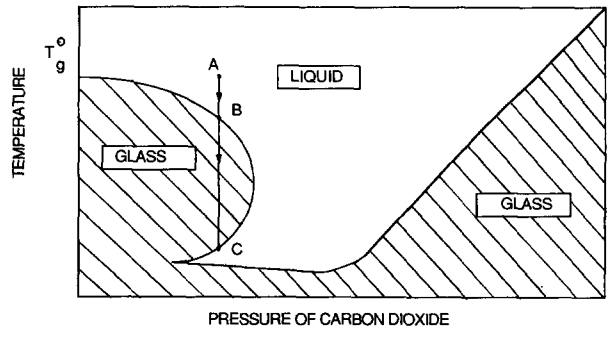

Figure 1 Hypothesis of glass–liquid transition for polymer–gas mixture

* To whom correspondence should be addressed

0032-3861/93/071410-08

polymer lies in equilibrium with a large excess of CO_2, and at constant CO_2 pressure, if the temperature is lowered from point A, the polymer will vitrify at point B due to a decrease in free volume upon decreasing temperature. However, as the temperature continues to decrease at constant pressure, the equilibrium solubility of CO_2 in the polymer tends to increase (as CO_2 density increases) which could ultimately lead to a glass–liquid transition at lower temperatures (point C). Previous work concerning liquid–liquid phase separation behaviour in polymer–CO_2 mixtures confirms that CO_2 sorption increases as temperature decreases at constant pressure[12,13], that is, lower critical solution temperature (LCST)-type phase boundaries. The general shape of the glass–liquid boundary in this region is consistent with the measurements by Wissinger and Paulaitis for the CO_2–PMMA system, as well as predictions by Johnston *et al.*[14] using the Sanchez–Lacombe equation of state and a free volume concept for T_g. It is important to remember that whereas the T_g–P_{CO_2} curve appears quite complex, a graph of T_g *versus* weight fraction CO_2 absorbed decreases monotonically, as expected[15].

Returning to *Figure 1*, moving to lower temperatures from point C at constant pressure, vitrification again occurs, regardless of pressure, due to decreasing thermal energy (and thus free volume) as well as the potential for upper critical solution temperature (UCST)-type liquid–liquid phase separation. Experience has shown that polymer–SCF systems will display hourglass type phase behaviour in temperature–concentration space[16], suggesting that the sorption of gas in the polymer will reach a maximum as the temperature decreases. Further decrease in temperature will decrease gas solubility, which, coupled with decreasing thermal energy, vitrifies the system. This portion of the glass–liquid boundary may exhibit a slightly negative slope because increasing pressure generally elevates the LCST and depresses the UCST (while also decreasing free volume, however).

Vitrification also occurs at higher pressures due to the effect of hydrostatic pressure on free volume and achievement of an effective maximum in gas sorption. The relative positions and shapes of the various parts of the glass–liquid boundary will vary according to specific aspects of the polymer–gas system, such as dT_g/dP for the pure polymer, ΔG_M, and the degree of sorption by glassy polymer. Thus it is conceivable that a pressure range exists where the polymer exhibits liquid-like behaviour at temperatures far below the ordinary glass transition temperature.

An understanding of the effect of gas pressure on T_g is important in the processing of foamed thermoplastics, particularly if one desires to minimize the thermal energy input required. We have studied the plasticization of PMMA networks by CO_2 using a dielectric method, and have compared these results to predictions of free volume in the networks as a function of pressure as calculated using a mean-field lattice gas model, modified to account for the elastic free energy.

THEORY

Model for swelling of networks by gases

A mean-field lattice gas (MFLG) model has been used to describe the free energy of mixing with an additional term to account for the elastic free energy. This allows good predictions of the swelling of polymer networks by gases as a function of pressure and temperature. Model equations have been described previously[17], thus only a brief summary is presented here.

The MFLG model[18] for the free energy of mixing assumes a pure component to be a binary mixture of segments and vacancies, or holes, on a lattice. Changes in the volume of the system are reflected by changes in the concentration of holes. Segments and holes are permitted different effective coordination numbers via the introduction of segmental contact surface areas as material parameters. The internal energy of mixing is derived using regular solution theory and surface fractions, instead of the usual volume fractions. The elastic free energy is calculated using Flory's derivation[19].

The free energy expression is used to derive the chemical potentials, which are subsequently employed to calculate the degree of swelling of the network by the gas using:

$$\mu_1^{I} = \mu_1^{II} \tag{1}$$

$$\mu_0^{I} = \mu_0^{II} \tag{2}$$

where the subscripts 0 and 1 refer to chemical potentials of the holes and solvent segments, and superscripts I and II refer to pure CO_2 and swollen polymer phases.

Because a system of methyl methacrylate repeat units, CO_2, holes and trifunctional methacrylate crosslinkers is employed, the system should be modelled as a quaternary. However, to simplify the mathematics the system was treated as a ternary with the following provisions:

1. The energetic material parameters for the crosslinker are assumed to be identical to those of the monomer.
2. The number of segments/molecule (m_x) and the surface area parameter (γ_x) for the crosslinker can be calculated using the derived values for the repeat unit (m_1, γ_1) and:

$$m_x = \frac{m_1 V_x}{V_1} \tag{3}$$

$$\frac{m_x M_x^0 (1-\gamma_x)}{m_1 M_1^0 (1-\gamma_1)} = \frac{S_x}{S_1} \tag{4}$$

where M_x^0 and M_1^0 are the molecular weights of the crosslinks and repeat units, V_x and V_1 are the molecular volumes of the crosslinks and repeat units, and S_x and S_1 are the molecular surface areas. The molecular volumes and surface areas are calculated using Bondi's group contribution method[20]. The values of m and γ for the network are subsequently calculated as segment fraction averages of m_1, m_x and γ_1, γ_x.

Dielectric relaxation in polymers

The dependence of the complex dielectric constant (ε^*) on frequency (ω) for a polymer having a single relaxation time is given by Debye's equations[21]:

$$\varepsilon^*(\omega) = \varepsilon'(\omega) - i\varepsilon''(\omega) \tag{5a}$$

$$\varepsilon'(\omega) = \varepsilon_\infty + \frac{\varepsilon_s - \varepsilon_\infty}{1+\omega^2\tau^2} \tag{5b}$$

$$\varepsilon''(\omega) = (\varepsilon_s - \varepsilon_\infty)\frac{\omega\tau}{1+\omega^2\tau^2} \tag{5c}$$

$$\tan\delta = \frac{\varepsilon''(\omega)}{\varepsilon'(\omega)} = \frac{(\varepsilon_s - \varepsilon_\infty)\omega\tau}{\varepsilon_s + \varepsilon_\infty\omega^2\tau^2} \tag{5d}$$

where ε_s is the steady-state value of $|\varepsilon^*|$ when the polymer

molecules are completely relaxed (at very low frequencies) and ε_∞ is the value of $|\varepsilon^*|$ at short times (at very high frequencies) when the polymer molecules are completely unrelaxed.

Equations (5a)–(5d) are based only on the dipolar contribution to the polarization and are also valid only for polymers having a single relaxation time. Therefore, they do not completely explain the behaviour of real polymers which have a distribution of relaxation times and also have mechanisms other than dipole orientation contributing to their dielectric behaviour. Molecular mechanisms giving rise to polarization can be categorized as bulk effects and interfacial effects[22]. The most important bulk mechanism other than dipole orientation is the bulk conductivity due to ionic mobility.

PMMA, being a polar polymer, has a relatively high equilibrium level of moisture. Further, washing the monomer (to remove inhibitor) with aqueous sodium hydroxide will lead to contamination with trace amounts of sodium ions. The presence of moisture or other ionic impurities (at ppm levels) in the sample leads to mobile charged species, the transport of which in an applied electric field produces an ionic contribution to both ε' and ε''. By including this ionic contribution, the dielectric loss factor and storage component can be described in a more general form[23] as:

$$\varepsilon'_{\text{apparent}} = \varepsilon'_{\text{dipolar}} + \varepsilon'_{\text{ionic}} \tag{6}$$

$$\varepsilon''_{\text{apparent}} = \varepsilon''_{\text{dipolar}} + \varepsilon''_{\text{ionic}} \tag{7}$$

where the ionic contributions are also frequency dependent. Uemura's model[24] for diffusion-controlled translational motion of ions in high-molecular-weight polymers predicts that at low frequencies:

$$\varepsilon'_{\text{ionic}} \propto (\omega)^{-3/2} \tag{8}$$

$$\varepsilon''_{\text{ionic}} \propto (\omega)^{-1} \tag{9}$$

Theoretically, ionic conductivity, σ, can be related to the number of charge carriers, n_i, their charge, q_i, and their mobility, μ_i, by the expression:

$$\sigma = \sum n_i q_i \mu_i \tag{10}$$

When these types of charge transport or charge polarization effects are absent, the fundamental definition relating the conductivity σ to ε'' is valid[22,23]:

$$\varepsilon''_{\text{ionic}} = \frac{\sigma}{\varepsilon_0 \omega} \tag{11}$$

where ε_0 is the permittivity of free space (8.85×10^{-14} farads cm^{-1}). As can be seen from equation (5c), at very low frequencies $\varepsilon''_{\text{dipolar}}$ becomes zero, and thus the contribution of ionic mobility dominates at low frequencies. A plot of $\log \varepsilon''$ *versus* $\log \omega$ at low ω should give a straight line of slope -1, with ionic conductivity (σ) derived from the intercept of the plot.

EXPERIMENTAL

Network synthesis and sample preparation

Methyl methacrylate monomer (Aldrich) and trimethylopropane trimethacrylate (Aldrich) were washed with 5 wt% NaOH solution to remove the inhibitor. In a typical experiment, 5 ml MMA, 0.1 ml TMA and 5 mg azobis(isobutyronitrile) (AIBN, Polysciences) are added to a 21×70 mm glass vial. Polymerization is initiated under N_2 by using 365 nm ultraviolet (u.v.) light (Spectronics Corporation model MB-100) at a distance of 12 cm from the surface of the reaction mixture. Single-piece dielectric sensors were embedded into the solid polymer network by dipping them into the reaction mixture and polymerizing *in situ*. After the reaction was complete, indicated by the solidification of the reaction mass, in $\approx$2–3 h, the samples were dried at 50–60°C in a vacuum oven overnight, and then removed from the glass vials.

Dielectric measurements

The experimental set-up used for making high-pressure dielectric measurements is shown schematically in *Figure 2*. A two-part conductive silver–epoxy (AI Technology, Prima Solder™ EG 8020HC) was used for soldering the sensor to the 20 gauge single-strand electric wires which connect it to the impedance analyser (Hewlett Packard 4192 LF). The epoxy was allowed to cure at room temperature for 24 h to achieve a high current-carrying capacity. The polymer sample was then enclosed in a stainless steel high-pressure window cell[25] designed for operation up to 15 000 psi (103.5 MPa) and fitted with sapphire windows. The impedance analyser is interfaced to a computer using software (FDEMS) developed by Dek-Dyne Inc. The cell is pressurized with CO_2 (Linde, bone dry), which has been purified through 3A molecular sieves, using a syringe-type manual pressure generator (cylinder capacity 30 cm^3, model 62-6-10, from High Pressure Equipment Co., Erie, PA, USA). The temperature of the cell is controlled to within $\pm$0.5°C by a programmable PID controller (CN-2000, Omega Engineering, Stamford, CT, USA). The pressure signal from the cell is converted to an electric signal by a pressure transducer and indicated on a digital display.

In a typical experiment, the cell is flushed with CO_2 for several minutes and then the pressure is increased in steps of 200 psi (1.4 MPa) while the temperature is held at 40°C. At each pressure, dielectric data is obtained simultaneously at several desired frequencies in the range 5 Hz to 10^6 Hz. Similarly, in temperature scans, after flushing with CO_2, the pressure is maintained at 0 psig and the temperature is raised in steps of 10°C.

The FDEMS software provides a calculation of ε' and ε'' *versus* ω from the measured capacitance and conductance of the sample. Average values of ε' and ε'' at each CO_2 pressure (or at each temperature) can therefore be obtained for an entire set of frequencies.

RESULTS AND DISCUSSION

Predictions of swelling of PMMA networks by supercritical CO_2

The pure component MFLG parameters for uncrosslinked PMMA and CO_2 were taken from the literature[18]. Binary interaction parameters for the CO_2–uncrosslinked PMMA mixture were found by fitting of the appropriate model equations (see, for example, ref. 18), to sorption data by Wissinger and Paulaitis[12], who measured both the volume change on swelling and the weight fraction of CO_2 absorbed at three different temperatures. Parameters are shown in *Table 1*. The quality of the model fit to the data is shown in *Figures 3* and *4*. Because the MFLG model is an equilibrium description, it will not accurately model the sorption of a gas by a glassy polymer. Thus the predictions of swelling at low pressures are only estimates as it is expected that the polymer is

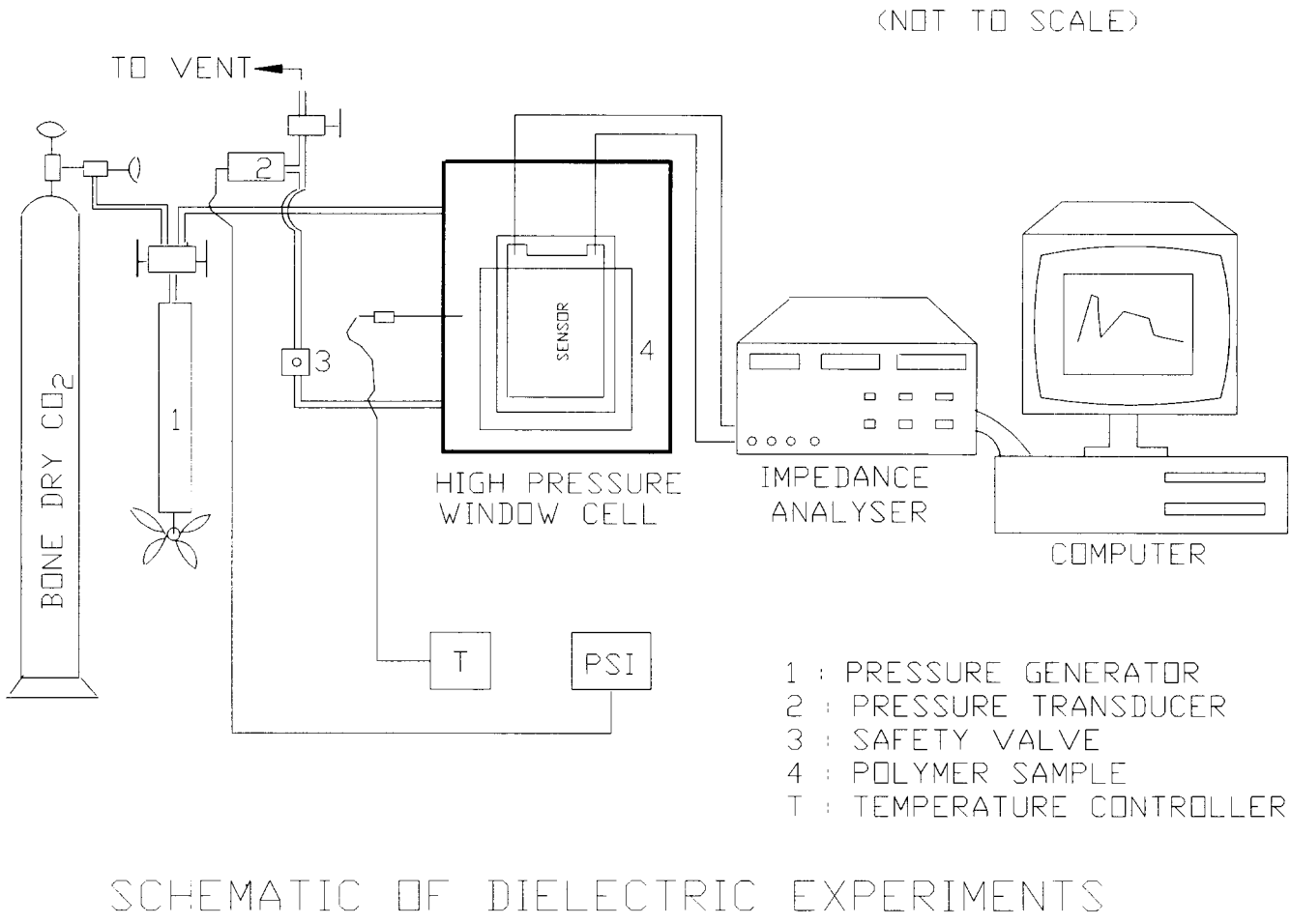

Figure 2 Schematic representation of experimental set-up for dielectric measurements at high pressures

Table 1 MFLG paramters for CO_2 and poly(methyl methacrylate)

Parameter	CO_2	PMMA
m^a	1.31	3.13
α	0.91498	−9.0493
g_{10}	−1.1445	6.1068
g_{11}	519.82	1361.0
γ	−1.2010	−1.2860

Parameters are defined in ref. 17
[a] Segments per monomer unit

Table 2 MFLG parameters for CO_2–PMMA mixture

Parameter	CO_2–PMMA
g_{m0}	−2.6832
g_{m1}	−70.209
α_m	7.6845

Parameters are defined in ref. 17

still glassy. As can be seen in *Figures 3* and *4*, the model reproduces very well the trends in both the volume change and the weight fraction of CO_2 absorbed. However, it tends to overpredict the amount of CO_2 absorbed at pressures higher than 800–1000 psi (551.5–689.4 MPa), which could be due partially to overestimation of pure CO_2 density by the model[17]. Given the necessary pure component and binary parameters, predictions of the degree of swelling of the PMMA networks in this study by CO_2 were made *versus* temperature, pressure, and crosslinker concentration using equations (1) to (4).

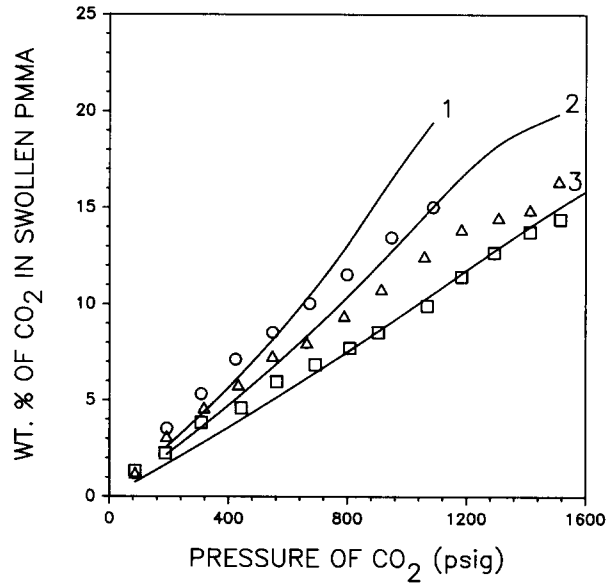

Figure 3 Experimental data (○, △, □) and model predictions (curves 1, 2, 3) of weight fraction CO_2 absorbed by PMMA as a function of pressure at three different temperatures; curve 1 and (○), 32.7°C; curve 2 and (△), 42.0°C; curve 3 and (□), 58.8°C. (1 psig = 6.895×10^3 Pa)

While there are no data for comparison, model predictions for the crosslinked PMMA networks show the expected trends, as seen in *Figures 5* and *6*. Both the volume fraction of holes and the amount of

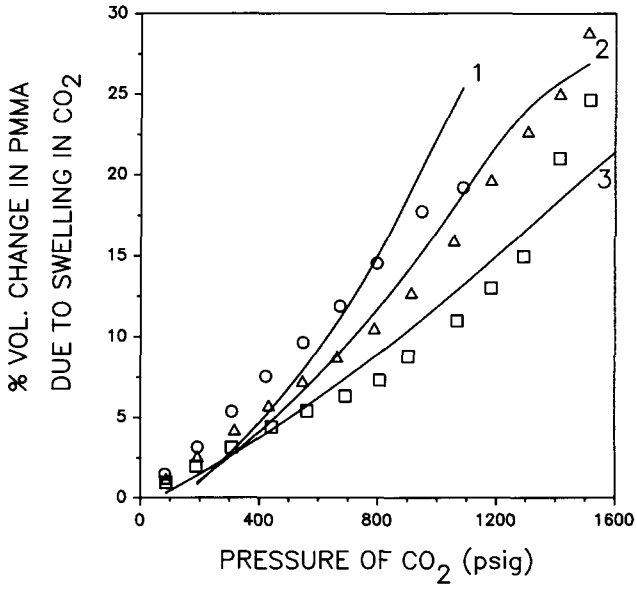

Figure 4 Experimental data (○, △, □) and model predictions (curves 1, 2, 3) of fractional volume change of PMMA as a function of CO_2 pressure at three different temperatures; curve 1 and (○), 32.7°C; curve 2 and (△), 42.0°C; curve 3 and (□), 58.8°C. (1 psig = 6.895×10^3 Pa)

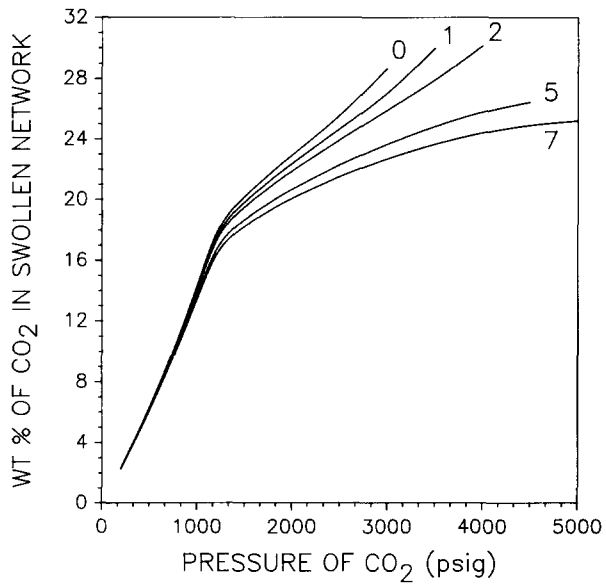

Figure 5 Model predictions of wt% CO_2 absorbed in PMMA networks as a function of gas pressure and vol% crosslinker (indicated by numerals on curves). (1 psig = 6.895×10^3 Pa)

absorbed CO_2 in the network increase with increasing CO_2 pressure. Also, swelling decreases with increasing crosslinker content at a given pressure. However, in all cases, the predicted absolute change in swelling as a function of CO_2 pressure is greater at pressures below 1200–1400 psi (8.272–9.652 MPa) than at higher pressures, which can be explained by the increasing importance of hydrostatic compression at higher gas pressures, as well as the reduced CO_2 compressibility (solubility of CO_2 in PMMA and other polymers correlates very well with gas density). This effect is more significant for highly crosslinked networks.

Dielectric relaxations

Figure 7 shows the los factor (ε'') for a 2% crosslinked network. The nature of the curves is quite different from the single peak maxima suggested by Debye's equations, which are due primarily to bulk conductivity. To see the finer details of the curves, more experimental data were obtained in the intermediate frequency range and are plotted in *Figure 8*. This figure exhibits features which are similar to the behaviour reported by Senturia and Shepard[22] for samples in which ionic conductivity contributes significantly to the dielectric response. The value of ε'' shows a simple maximum against ω for relaxations governed only by dipole orientation (equation (5b)), but with increasing contribution of ionic mobility, very high values of ε'' are seen at low frequencies and the dipolar maximum reduces to a small shoulder in the curve. This suggests that the total response of these samples is the sum of two different contributions: a linear curve at lower frequencies (conductivity) and a small peak

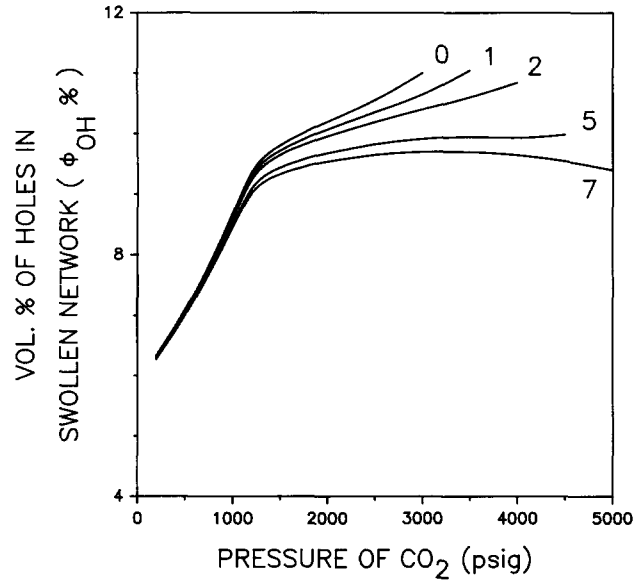

Figure 6 Model predictions of vol% holes in PMMA networks swollen by CO_2 as a function of gas pressure and vol% crosslinker (indicated by numerals on curves). (1 psig = 6.895×10^3 Pa)

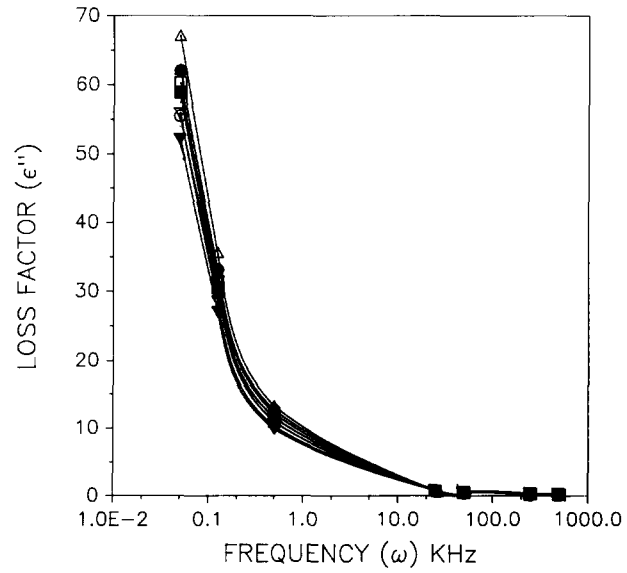

Figure 7 Loss factor ε'' *versus* frequency ω for PMMA network at 40°C and eight different gas pressures; 2% crosslinker; (○) 0; (●) 600; (△) 1200; (▲) 2000; (□) 3000; (■) 4000; (▽) 5000; and (▼) 5800 psig. (1 psig = 6.895×10^3 Pa)

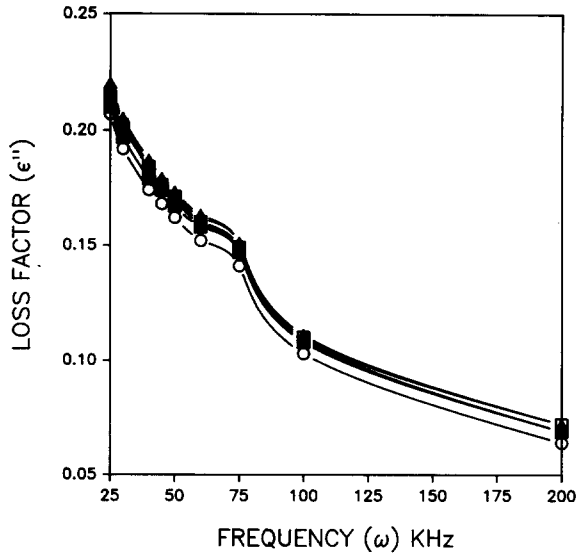

Figure 8 Medium frequency range details of loss factor (ε'') *versus* frequency (ω) for PMMA network at 40°C and six different gas pressures; 2% crosslinker; (○) 0; (●) 600; (△) 1000; (▲) 2000; (□) 3000; and (■) 4000 psig. (1 psig = 6.895×10^3 Pa)

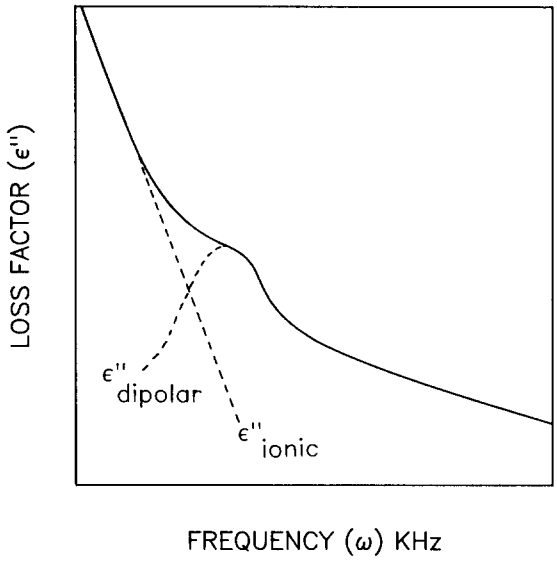

Figure 9 Ionic and dipolar contributions to the dielectric loss factor, ε''

at higher frequencies (dipolar relaxation) which is partly hidden behind the linear curve (*Figure 9*).

To test this interpretation, we have used the expression for frequency dependence of ε''_{ionic} as given by equation (9). According to this equation, $\log \varepsilon''$ *versus* $\log \omega$ should be a straight line if the conductivity contribution dominates at low ω. This has been found to be true for our data in the frequency range 5–100 Hz with a linear correlation coefficient of >0.99 and slopes close to -1, as given by equation (9).

The values of ionic conductivity at different CO_2 pressures were obtained as σ/ε_0 from the intercepts of the linear regression. We have used the value of σ at 0 psig and 40°C (σ_0) to normalize the values of ionic conductivities at different pressures and the reduced values thus obtained are plotted as σ/σ_0 against pressure of CO_2 in *Figures 10* and *11*.

The maximum (at $\approx$1200 psi (8.272 MPa) pressure) in *Figure 10* can be explained by the concept of free volume in polymer systems. At constant temperature, two factors which affect the free volume of our system are hydrostatic compression of the sample, which tends to decrease the free volume, and absorption of CO_2 in the network (itself a function of pressure), which tends to increase the free volume. Thus, there are two competing effects. At lower pressures, the degree of swelling of the network by CO_2 increases rapidly as the pressure increases and is more important than the hydrostatic compression. The free volume of the sample consequently increases with increasing pressure, leading to an increase in the mobility of ionic impurities and thus an increase in the value of σ. As pressure is increased above 1200 psig (8.272 MPa), swelling eventually reaches a maximum value for the crosslinked networks due to elastic constraints and a decrease in CO_2 compressibility, and compression of the sample becomes increasingly important. Further increases in pressure beyond this point lead to a

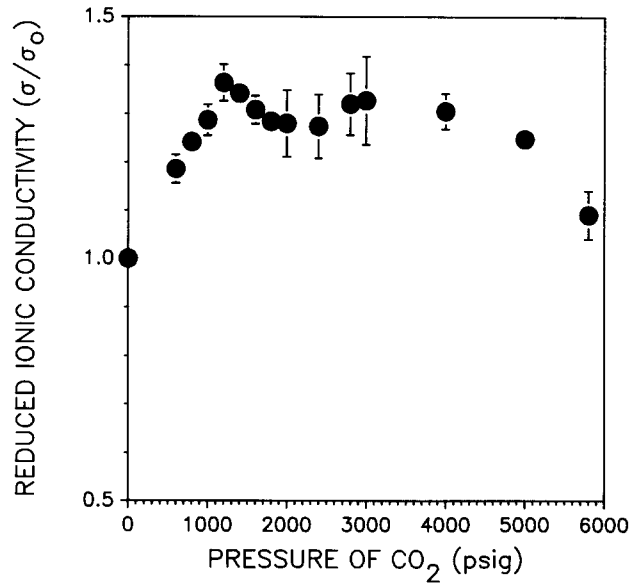

Figure 10 Reduced ionic conductivity (σ/σ_0) for PMMA network as a function of gas pressure at 40°C; 2% crosslinker. (1 psig = 6.895×10^3 Pa)

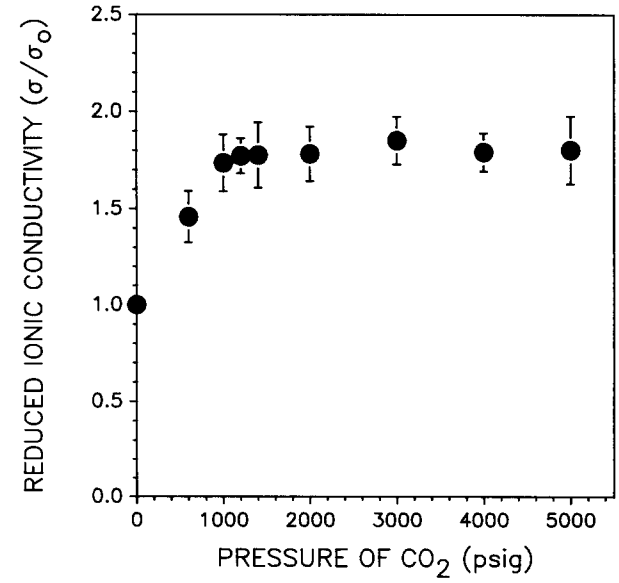

Figure 11 Reduced ionic conductivity (σ/σ_0) for uncrosslinked PMMA as a function of gas pressure at 40°C. (1 psig = 6.895×10^3 Pa)

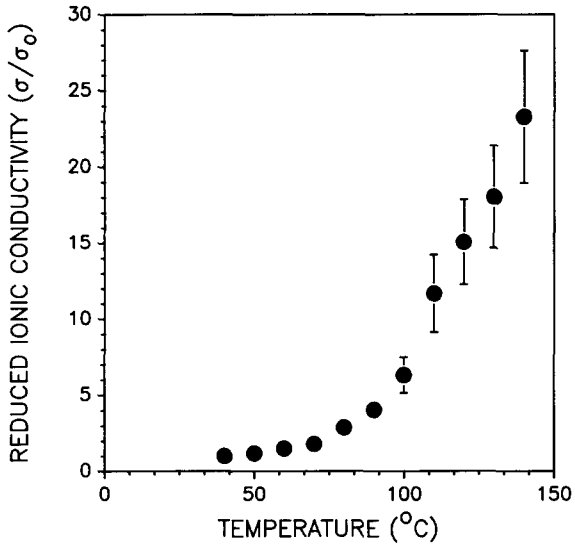

Figure 12 Reduced ionic conductivity (σ/σ_0) for PMMA network as a function of temperature at gas pressure of 0 Pa; 2% crosslinker

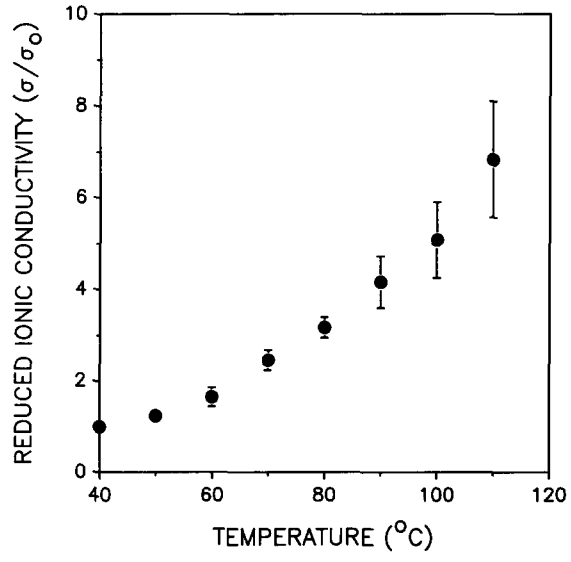

Figure 13 Reduced ionic conductivity for uncrosslinked PMMA as a function of temperature at a gas pressure of 0 Pa

decrease in free volume and consequently a decrease in the value of σ. In the case of uncrosslinked PMMA (*Figure 11*), there are no constraints on the swelling of the polymer and therefore there is no maximum seen in the mobility curve. However, σ/σ_0 reaches a plateau in approximately the same pressure range of 1200–1400 psi (8.272–9.652 MPa). This suggests that the rate of swelling with pressure undergoes a sharp change in this pressure range. Our model predictions (*Figures 5* and *6*) show the same trend.

In a similar way as in pressure scan experiments, ionic conductivities for pure PMMA and crosslinked PMMA networks have been calculated as a function of temperature, while maintaining the gas pressure at 0 psig. Dimensionless conductivities are obtained by dividing by the value at 40°C. Results are shown in *Figures 12* and *13*. These show a monotonically increasing trend with temperature which is expected because of the increase in free volume with temperature. By comparing *Figures 10* and *11* with *Figures 12* and *13*, a correspondence can be established between the effect of temperature and that of CO_2 pressure in plasticizing the polymer.

The shoulder of the maxima peak in ε'' *versus* ω curves at higher frequencies (*Figure 8*) can be analysed using the information that dielectric loss peaks are associated with either the glass transition or local reorientation processes[26]. In PMMA, the occurrence of two well resolved major peaks (α and β) has been observed[26]. Williams[27] has reported a large β peak with an indication of a small α peak for conventional atactic PMMA. The β peak is often associated with the hindered rotation of the side group about the C–C bond linking it to the main chain[28].

Although our ε' *versus* temperature data at low frequencies (*Figure 14*) agrees with the behaviour reported in literature (Figure 8.17 of ref. 26), the high-frequency dipolar peak observed by us occurs at a frequency much higher than those reported for α and β relaxations of PMMA. At 40°C, the α peak of PMMA is seen at a frequency close to 10 Hz and the β peak at approximately 100 Hz (Figure 8.8 of ref. 26). In this frequency range, conductivity dominates the dielectric behaviour of our samples, and we are not able to observe any of these peaks. The dipolar peak observed by us at about 75 kHz (low-temperature relaxation) can be attributed to the relaxation of the trimethacrylate crosslink units. Low-temperature relaxation in the same frequency range has also been reported in the literature for poly(ethyleneglycol methacrylate) and poly(diethyleneglycol mehacrylate)[29]. Some interesting insight can be gained by examining this peak more closely (*Figure 15*). As can be seen, the magnitude of this 'shoulder' increases with increasing pressure, indicating the increasing degree of plasticization as pressure increases[7], until a maximum is reached somewhere between 1000 and 2000 psi (6.894 and 13.793 MPa). At pressures $\geqslant$2000 psi ($\geqslant$13.793 MPa), increases in pressure decrease the magnitude of the peak, consistent with the ionic conductivity results and also with the hypothesis that hydrostatic compression plays an increasingly important role above 1200–1400 psi (8.272–9.652 MPa) in the CO_2/PMMA mixture at 40°C.

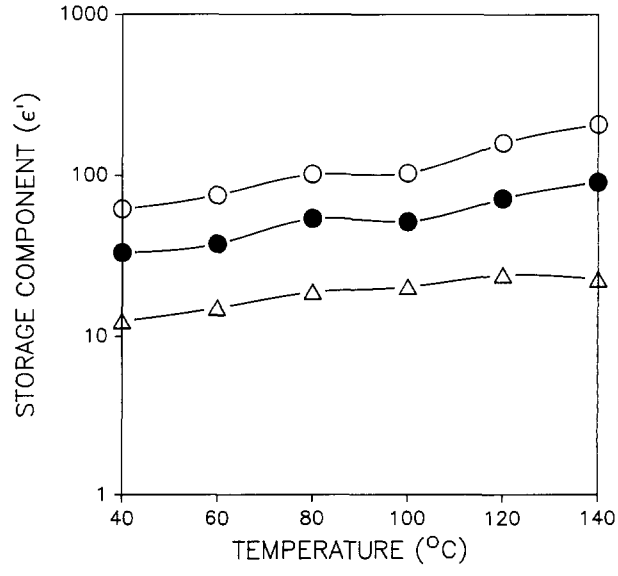

Figure 14 Storage component ε' *versus* temperature for PMMA network at CO_2 pressure of 0 Pa; 2% crosslinker. (○) 0.05; (●) 0.125; and (△) 0.5 kHz

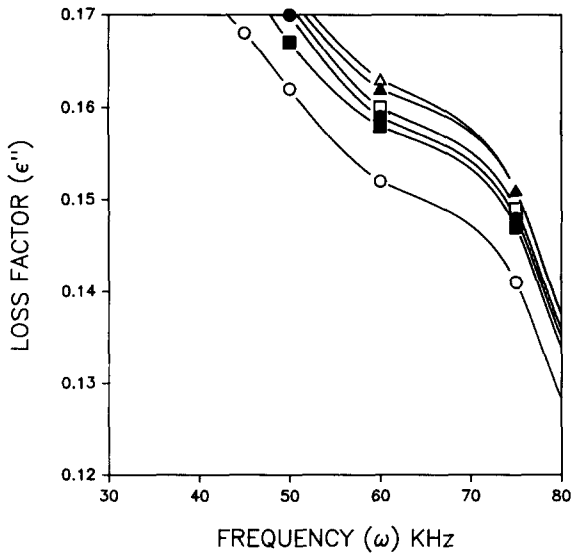

Figure 15 Low-frequency portion of *Figure 8* enlarged to show the magnitude of the β-relaxation peak *versus* pressure; (○) 0; (●) 600; (△) 1000; (▲) 2000; (□) 3000; and (■) 4000 psig. (1 psig = 6.895×10^3 Pa)

CONCLUSIONS

In the study of dielectric relaxations in PMMA networks swollen by CO_2, two major contributions to the dielectric behaviour have been observed. Ionic conductivity plays a significant role at lower frequencies and dipolar effects are dominant only at higher frequencies. Results show that the ionic conductivity (and thus the viscosity of the matrix at the molecular level) increases with increasing CO_2 pressure up to approximately 1200 psi (8.272 MPa), levelling out (or decreasing) at higher pressures. With increasing temperature, the ionic conductivity shows a monotonously increasing trend as expected. These trends are entirely consistent with predictions, using a modified lattice model, of the free volume in the swollen networks *versus* pressure. The magnitude of the dipolar relaxation peak, which reflects the degree of plasticization of the polymer sample by CO_2, also exhibits a maximum *versus* pressure, also between 1000 and 2000 psi (6.894 and 13.793 MPa). These results illustrate the counteracting effects of hydrostatic compression and CO_2 absorption on the plasticization of the networks, and the effect of pressure on each factor. The MFLG model, modified to include the elastic free energy, provides a good description of the effect of pressure on the swelling of PMMA by CO_2.

ACKNOWLEDGEMENTS

The authors gratefully acknowledge the financial support of the National Science Foundation (CTS-9005155) and the Petroleum Research Fund (ACS-PRF No. 22901-G7) for this work.

REFERENCES

1 McHugh, M. A. and Krukonis, V. J. 'Supercritical Fluid Extraction', Butterworths, Stoneham, MA, 1986
2 Beckman, E. J. and Porter, R. S. *J. Polym. Sci., Polym. Phys. Edn* 1987, **25**, 1511
3 Traenckner, H. J., Lolhr, K. D., Wehnert, W., Wulff, C., Arlt, W. and Paul, H. I. *Eur. Pat. Appl.* No. 356 815, 7 March 1990
4 Hachisuka, H., Sato, T., Imai, T., Sujita, Y. T., Takizawa, A. and Kinoshita, T. *Polym. J.* 1990, **22**, 77
5 Wang, W. V., Kramer, E. J. and Sachse, W. H. *J. Polym. Sci., Polym. Phys. Edn* 1982, **20**, 1371
6 Wissinger, R. G. and Paulaitis, M. E. *J. Polym. Sci., Polym. Phys. Edn* 1991, **29**, 631
7 Kamiya, Y., Mizoguchi, K. and Naito, Y. *J. Polym. Sci., Polym. Phys. Edn* 1990, **28**, 1955
8 Chiou, J. S., Barlow, J. W. and Paul, D. R. *J. Appl. Polym. Sci.* 1985, **30**, 2633
9 Chiou, J. S., Maeda, Y. and Paul, D. R. *J. Appl. Polym. Sci.* 1985, **30**, 4019
10 Sefcik, M. D. and Schaefer, J. *J. Polym. Sci., Polym. Phys. Edn* 1983, **21**, 1055
11 Sefcik, M. D. *J. Polym. Sci., Polym. Phys. Edn* 1986, **24**, 957
12 Wissinger, R. G. and Paulaitis, M. E. *J. Polym. Sci., Polym. Phys. Edn* 1987, **25**, 2497
13 Lian, I. S. and McHugh, M. A. in 'Supercritical Fluid Science and Technology' (Eds J. M. L. Penninger, M. Radosz, M. A. McHugh and V. J. Krukonis) Elsevier, Amsterdam, 1985, pp. 415–434
14 Johnston, K. P., Dixon, D. and Condo, P. AIChE Annual Meeting, Los Angeles, CA, November 1991, Paper no. 205e
15 Kalospiros, N. S. and Paulaitis, M. E. AIChE Annual Meeting, Los Angeles, CA, November 1991, Paper no. 45d
16 Zerman, L. and Patterson, D. *J. Phys. Chem.* 1972, **76**, 1214
17 Goel, S. K. and Beckman, E. J. *Polymer* 1992, **33**, 5032
18 Beckman, E. J., Koningsveld, R. and Porter, R. S. *Macromolecules* 1990, **23**, 2321
19 Flory, P. J. *J. Chem. Phys.* 1977, **66**, 5720
20 Bondi, A. 'Physical Properties of Molecular Crystals, Liquids, and Glasses', John Wiley, New York, 1968
21 Aklonis, J. J. and MacKnight, W. J. 'Introduction to Polymer Viscoelasticity', John Wiley, New York, 1982
22 Senturia, S. D. and Shepard Jr, N. F. *Adv. Polym. Sci.* 1986, **80**, 1
23 Kranbuehl, D. E., Delos, S. E. and Jue, P. K. *Polymer* 1986, **27**, 11
24 Uemura, S. *J. Polym. Sci., Polym. Phys. Edn* 1974, **12**, 1177
25 Goel, S. K. *MS Thesis*, University of Pittsburgh, 1991
26 McCrum, N. G., Read, B. E. and Williams, G. 'Anelastic and Dielectric Effects in Polymeric Solids', John Wiley, New York, 1967
27 Williams, G. *Trans. Faraday Soc.* 1966, **62**, 2091
28 Ku, C. C. and Liepins, R. 'Electrical Properties of Polymers — Chemical Principles', Hanser, Munich, 1987
29 Bares, J. and Janacek, J. *Coll. Czech. Chem. Commun.* 1965, **30**, 1604